VNU Journal of Science: Mathematics – Physics, Vol. 38, No. 1 (2022) 58-64

VNU Journal of Science: Mathematics - Physics

Journal homepage: https://js.vnu.edu.vn/MaP

Original Article

Effect of Eu Doping on Structural, Optical and Magnetic Properties of $BiFeO_3$ Materials

Dao Viet Thang[1,2,*], Nguyen Manh Hung[1,2], Nguyen Phuong Thao[2], Nguyen Cao Khang[2], Le Thi Mai Oanh[2], Ngo Thi Cam Linh[3], Bui Dinh Tu[4]

[1]*Hanoi University of Mining and Geology, 18 Vien Street, Duc Thang Ward, North Tu Liem, Hanoi, Vietnam*

[2]*Center for Nano Science and Technology, Hanoi National University of Education, 136 Xuan Thuy, Cau Giay, Hanoi, Vietnam*

[3]*Military University of Culture and Art, 101 Nguyen Chi Thanh, Dong Da, Hanoi, Vietnam*

[4]*VNU University of Engineering and Technology, 144 Xuan, Cau Giay, Hanoi, Vietnam*

Received 18 March 2021
Revised 28 July 2021; Accepted 15 August 2021

Abstract: $Bi_{1-x}Eu_xFeO_3$ (BEFO) (x = 0.00 ÷ 0.10) materials were prepared by sol-gel method. The crystal structural, Raman scattering, magnetic and optical properties of BEFO were investigated by X-ray diffraction (XRD), Raman scattering spectroscopy, magnetic hysteresis (M-H) loops and fluorescence spectroscopy (FL), respectively. Obtained results of the characterization showed that Eu-doping affected structural, optical and magnetic properties of BFO materials. All samples were crystallized in the rhombohedral structure with R_{3C} space group with crystal lattice parameters of a = 5.585 Å, c = 13.832 Å and the average crystal size of L_{XRD} = 581 Å for BFO materials whereas the a, c and L_{XRD} of Eu-doped samples decrease with the increasing of Eu^{3+} concentration. The analysis result of Raman scattering spectroscopy showed that the position of the characteristic peak for Bi-O covalent bonds shifts toward higher frequency when Eu^{3+} concentration increases, confirming the dopping substitution of Eu^{3+} ions into Bi-sites. Fluorescence spectra showed the enhancement of characteristic emission peaks with the increase of Eu concentration. All samples exhibited weak ferromagnetic behaviour with saturation magnetization of M_s = 0.006 emu/g and remnant magnetization of M_r = 0.004 emu/g for BFO materials. The value of M_s and M_r of Eu-doped BFO increases compared to those of undoped-BFO. The origin of ferromagnetism and fluorescence improvement has been discussed.

Keywords: Fluorescence, ferromagnetic, Eu-doped, X-ray, Raman.

* Corresponding author.
E-mail address: daovietthang@humg.edu.vn

https//doi.org/10.25073/2588-1124/vnumap.4640

1. Introduction

Multiferroic materials are well known to contain ferroelectric and ferromagnetic (antiferromagnetic) orders simultaneously and exhibit ferroelastic and magnetoelectric (ME) effect in the same structure phase [1]. These materials have found broad applications in electronic devices such as information storage, memory, sensor, and in ultrasonic technologies. The multiferroic materials are very rare in nature because of the competition between the ferromagnetic and the ferroelectric orders. $BiFeO_3$ (BFO) was found to be one of the few multiferroic materials where the antiferromagnetic order (with Néel temperature T_N = 643 K) and the ferroelectric order (with Currie temperature T_C = 1100 K) coexist [2, 3]. Recent studies have showed that the optical properties of doped BFO materials can be applied for the next generation of smart materials. At room temperature, BFO crystallizes in a rhombohedral structure with R_{3C} space group [4, 5]. The rhombohedral structure may be obtained from a cubic parent perovskite by the rotation of the oxygen octahedra around the (111) direction and the displacement of Bi^{3+} and Fe^{3+} cations along the same *c* direction [6]. Fe^{3+} ions are located in the distorted oxygen octahedra, while Bi^{3+} ions, occupying the dodecahedron positions are strongly shifted from the central position towards one of Fe^{3+} ions due to the electron lone pair of Bi^{3+} effect.

Recently, some studies have shown the influence of impurity element, impurity concentration and fabrication conditions such as temperature and pressure on crystal structure and physical properties of the host BFO materials [7]. The studies indicated the strong dependence of magnetic properties on nanoscale structure [8]. For example, while BFO presents anti-ferromagnetic behaviour with G-type cycloid spin configuration with a period of 62 nm, BFO doped with rare earth (*RE*) ion exhibits an enhancement of both ferromagnetic and optical properties which are important requirement for the next generation of multifunctional devices. Some recent reports showed the effect of Eu^{3+} doping on the characteristics of $BiFeO_3$ powders produced by conventional techniques such as hydrothermal process and sol-gel method [9-13]. Even if the magnetic behaviours of Eu-doped BFO have been thoroughly analyzed, very few data regarding fluorescence has been reported.

Herein, we studied the effect of Eu^{3+} doping on the structural, magnetic and optical properties of BFO materials. In particular, the fluorescence data are carefully analyzed to show the enhancement in optical properties of the doped samples, which is beneficial for the fabrication of next-generation multifunction devices.

2. Experiment

Pure $BiFeO_3$ and Eu^{3+}-doped $BiFeO_3$ materials were synthesized by the sol-gel method. The initial chemicals were: $Bi(NO_3)_3.5H_2O$ (Sigma-Aldrich, 98%), $Fe(NO_3)_3.9H_2O$ (Sigma-Aldrich, 98%), $Eu(NO_3)_3.6H_2O$ (Sigma-Aldrich, 99,9%), ethylene glycol $C_2H_6O_2$ (Sigma-Aldrich, 98%), and citric acid $HOC(COOH)(CH_2COOH)_2$ (Sigma-Aldrich, 98%). Firstly, $Bi(NO_3)_3.5H_2O$, $Fe(NO_3)_3.9H_2O$ and $Eu(NO_3)_3.6H_2O$ were dissolved in 35 ml of citric acid solution. The solution was then magnetically stirred at temperature 60 °C for 45 minutes to obtain homogeneous solutions. Then, by heating the solutions up to temperature of 100 °C for 3 hours, water in the solution were evaporated and a wet gel was formed. The gel was dried at 130 °C for 4 hours to achievea condensed gel. Finally, the dry gel was annealed at temperature of 800 °C for 7 hours to get BFO powder materials.

The structural, magnetic and optical properties of all samples were investigated by using X-ray diffraction (Equinox 5000, Cu-Kα radiation), Raman scattering (LabRAM HR Evolution, λ = 532 nm), magnetization hysteresis loops (*M-H*, Lake Shore Cryotronics, 7404 VSM), and fluorescence emission spectroscopy (iHR550, Horiba, λ = 266 nm).

3. Results and Discussion

The phase formation and crystalline structure of $Bi_{1-x}Eu_xFeO_3$ materials (x = 0, 0.025, 0.05, 0.075, and 0.10) were investigated by XRD measurement. The XRD patterns of all samples are shown in Figure 1. The refinement of these patterns following the standard Cards JCPDS No. 71-2494 revealed that all samples exhibit rhombohedral structure. The main characteristic diffraction peaks belong to the (012), (104), (110), (006), (202), (024), (116), (122), (018), and (300) crystalline planes, as shown in Figure 1a. The XRD of BFO pure and Eu-doped $BiFeO_3$ samples show that Eu^{3+} ions are well incorporated into the BFO crystal lattice. Figure 1b shows a comparison of the positions of the (012), (104), and (110) peaks, which may depict the effect of Eu-doping on the crystalline structure of BFO. As it is seen, the corresponding peaks of the Eu-doped samples shift toward larger 2θ values compared to those of BFO. From XRD data, the crystal lattice parameters (a and c) and the average crystal size (L_{XRD}) have been determined by using the UnitCell software and Debye Sherrer's formula, and results are shown in Table 1. As seen in Table 1, the BFO pure sample has crystal lattice parameters of a = 5.585 Å, c = 13.832 Å and the average crystal size L_{XRD} = 58.1 nm. It is also seen that the crystal lattice parameters and the average crystal size of Eu-doped samples decrease when the concentration of Eu increases. This observation can be easily understood considering the smaller ionic radius of Eu^{3+} (1.07 Å) compared to that of Bi^{3+} (1.17 Å). When the Eu^{3+} ions are substituted into Bi-sites, the crystal lattice of the sample was a little bit contractive, resulting the decrease of the Bi/Eu-O bond length.. Furthermore, the Eu^{3+} ion with the small ionic radius is not large enough to fill 12-sided cavity created by the BO_6 octahedron causing the BO_6 octahedron to rotate, which reduces the 12-sided cavity volume. So, the Eu-doped $BiFeO_3$ samples with larger Eu ion concentrations, the rotation of BO_6 octahedron is significant leading to significant reduction of both the crystal lattice parameters of a and c. This is maybe the reason why the average crystal size L_{XRD} decreased , as shown in Table 1. The report of Park *et al*. [14] and Surdu *et al.* [15] also indicated that the crystal lattice parameters changed due to the difference in ionic radius of rare-earth ions and Bi^{3+} ions.

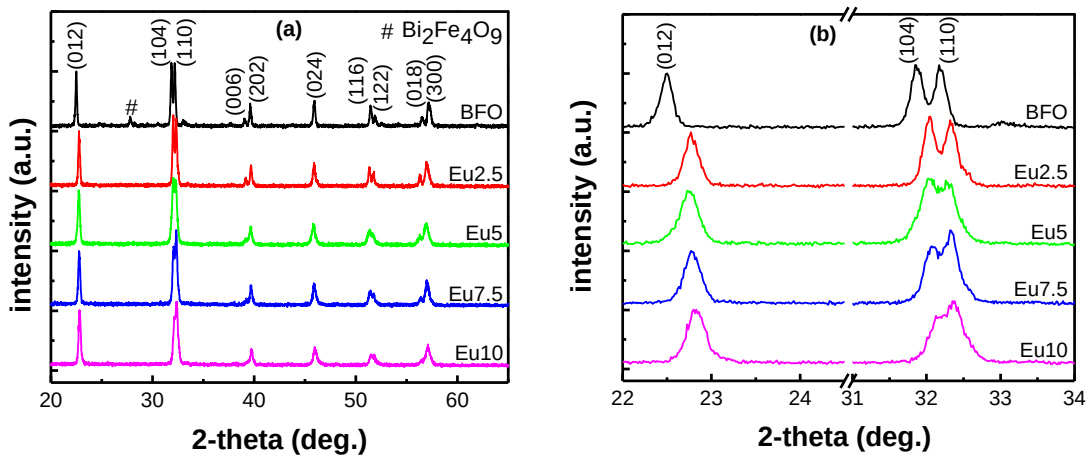

Figure 1. a) X-ray diffraction patterns of pure BFO and Eu-doped BFO materials; b) Magnification of (012), (104), and (110) diffraction peaks.

Table 1. The crystal lattice parameters (a and c) and the average crystal size L_{XRD} of BFO and Eu-doped $BiFeO_3$ samples.

Samples	a (Å)	c (Å)	L_{XRD} (nm)
BFO	5.585	13.832	58.1
Eu2.5	5.572	13.826	56.7
Eu5	5.570	13.820	49.4
Eu7.5	5.562	13.810	46.2
Eu10	5.555	13.787	43.9

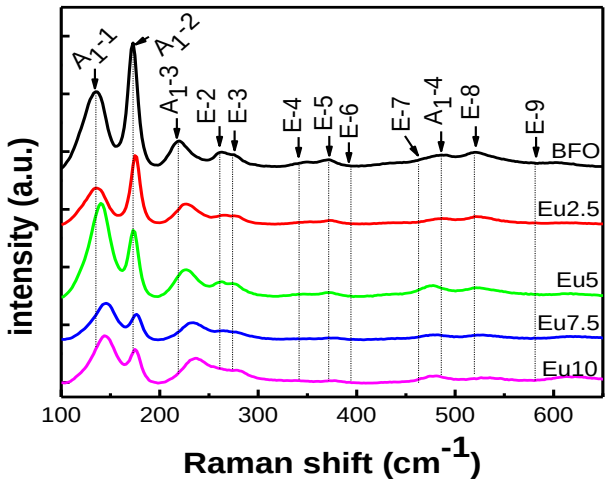

Figure 2. Raman scattering spectra of pure BFO and Eu-doped BFO materials.

Table 2. Raman modes observed and assigned by various research and Raman modes for BFO and Eu-doped $BiFeO_3$ samples.

Modes	Position of Raman modes (cm^{-1})					
	Yang et al., [18]	BFO	Eu2.5	Eu5	Eu7.5	Eu10
A_1-1	139	134	135	140	144	145
A_1-2	171	173	175	173	176	177
A_1-3	217	218	226	227	233	236
E-2	260	228	237	241	261	261
E-3	274	260	271	275	276	280
E-4	306	270	275	279	283	284
E-5	344	348	350	344	342	338
E-6	368	371	374	373	376	376
E-7	430	467	471	444	443	411
A_1-4	468	482	485	476	478	478
E-8	520	523	525	524	528	531
E-9	611	589	595	611	621	621

Raman scattering spectra of BFO and Eu-doped $BiFeO_3$ are shown in Figure 2. According to the group theory, 13 Raman active modes could be expected for the rhombohedral BFO structure with the R_{3C} space group ($\Gamma = 4A_1 + 9E$) [16, 17]. However, not all modes could be clearly observed at room

temperature. In the analysis of Raman scattering spectra for all samples, the position of Raman active modes for all samples are fitted by the Gaussian function, and results are presented in Table 2. As one can see in Table 2, for the Eu-doped BFO samples, there is a shift towards the higher frequencies in the position of the A_1-1, A_1-2, A_1-3, E-2, E-3, E-4, E-6, A_1-4, E-8, E-9 compared to the situations in the BFO sample. Previous studies have also shown that both the A_1 modes and the E modes at low frequencies are characteristic modes for the Bi-O covalent bonds, while other E modes at high frequencies are characteristic for the Fe-O bonds [9, 16]. Therefore, the A_1-1, A_1-2, A_1-3, E-2, E-3, E-4, E-6 and A_1-4 modes are found characteristic for the Bi-O covalent bonds and the E-8, E-9 modes are characteristic for the Fe-O bonds. The observed shift of the positions of A_1-1, A_1-2, A_1-3, E-2, E-3, E-4, E-6, A_1-4 modes showed that the Eu^{3+} ions are substituted into the Bi-sites. These results are consistent with the XRD results, confirming the substitution doping of Eu^{3+} ions into Bi-sites.

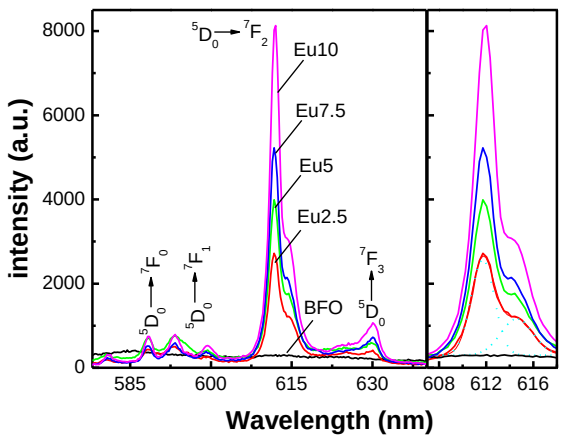

Figure 3. Fluorescence spectra of pure BFO and Eu-doped BFO materials.

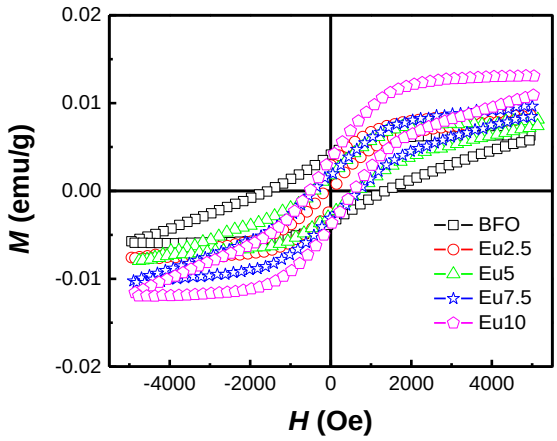

Figure 4. Magnetic hysteresis loops of BFO and Eu-doped $BiFeO_3$ materials.

Figure 4 shows the magnetic hysteresis loops of a pure BFO and Eu-doped BFO samples measured at room temperature. It is obvious that all samples exhibited weak ferromagnetic behaviour. The BFO sample has a saturation magnetization of M_s = 0.006 emu/g and a remnant magnetization M_r

= 0.004 emu/g. For the Eu-doped BFO samples, the M_s value increases from 0.008 to 0.013 emu/g while the M_r value slight changes when concentration of Eu^{3+} ions increase from 0.025 to 0.10, respectively. These results can be explained from the following considerations. The substitution of the Eu^{3+} ions into $BiFeO_3$ crystal lattice along with high temperature annealing of samples creates oxygen vacancies and lattice defects thereby contributing to the enhancement of the magnetization. In addition, the increase in Eu^{3+} concentration affects the spin spiral structure, most likely by a perturbation of the super-exchange interactions between localized Eu 4*f* and Fe 3*d* electrons. Some previous studies have also showed that the super-exchange interactions between localized *RE* 4*f* and Fe 3*d* electrons contributed in the enhancement of the magnetization of *RE*-doped $BiFeO_3$ materials [20-22].

4. Conclusion

In summary, both the pure $BiFeO_3$ and Eu-doped $BiFeO_3$ materials were successfully synthesized by the sol-gel method. XRD and Raman scattering investigation showed the substitution doping of Eu^{3+} ions into the Bi-sites in the host $BiFeO_3$ lattice. The most pronounced ferromagnetic behaviour was observed for Eu-doped $BiFeO_3$ samples with Eu^{3+} concentration of 10% molar which exhibited a saturation magnetization of $M_s \sim 0.013$ emu/g. This is most likely ascribed to the disorder of the super-exchange interactions between localized Eu 4*f* and Fe 3*d* electron. This study indicated a possibility to improve magnetic behaviour of $BiFeO_3$ using rare earth metal substitution into the A-site of the perovskite structure. In addition, the substitution of Eu^{3+} ions into Bi-sites of the host BFO materials enhanced the photoluminescence of the materials. This is a good sign for the search for new materials that are suitable for making next-generation multifunction devices.

Acknowledgement

This work is supported by Vietnam National Foundation for Science and Technology Development (NAFOSTED) under grant number 103.02-2018.34 and Hanoi University of Mining and Geology under grant number T22-18.

References

[1] W. Eerenstein, N. D. Mathur, J. F. Scott, Multiferroic and Magnetoelectric Materials, Nature, Vol. 442, 2006, pp. 759-765, https://www.readcube.com/articles/10.1038/nature05023.

[2] R. Mazumder, P. S. Devi, D. Bhattacharya, P. Choudhury, A. Sen, M. Raja, Ferromagnetism in Nanoscale $BiFeO_3$, Applied Physics Letters, Vol. 91, No. 6, 2007, pp. 062510, https://doi.org/10.1063/1.2768201.

[3] J. M. Moreau, C. Michel, R. Gerson, W. J. James, Ferroelectric Diffraction $BiFeO_3$ X-ray and Neutron Study, Journal of Physics and Chemistry of Solids, Vol. 32, No. 6, 1971, pp. 1315-1320, https://doi.org/10.1016/S0022-3697(71)80189-0.

[4] A. R. Makhdoom, S. M. Shah, T. Mahmood, M. J. Iqbal, M. J. Akhtar, M. A. Rafiq, Enhancement of Ferromagnetism by Suppression of Spiral Spin Structure in Ba Doped $BiFeO_3$, Journal of Magnetism and Magnetic Materials, Vol. 484, 2019, pp. 286-290, https://doi.org/10.1016/j.jmmm.2019.04.045.

[5] T. Tong, J. Chen, D. Jin, J. Cheng, Preparation and Gas Sensing Characteristics of $BiFeO_3$ Crystallites, Materials Letters, Vol. 197, 2017, pp. 160-162, http://dx.doi.org/10.1016/j.matlet.2017.03.091.

[6] B. Ruette, S. Zvyagin, A. P. Pyatakov, A. Bush, J. F. Li, V. I. Belotelov, A. K. Zvezdin, D. Viehland, Magnetic-Field-Induced Phase Transition in $BiFeO_3$ Observed by High-Field Electron Spin Resonance: Cycloidal to

Homogeneous Spin Order, Physical Review B, Vol. 69, 2004, pp. 064114, https://journals.aps.org/prb/abstract/10.1103/PhysRevB.69.064114.

[7] Z. Lin, W. Cai, W. Jiang, C. Fu, C. Li, Y. Song, Effects of Annealing Temperature on The Microstructure, Optical, Ferroelectric and Photovoltaic Properties of $BiFeO_3$ Thin Films Prepared by Sol–Gel Method, Ceramics International, Vol. 39, No. 8, 2013, pp. 8729-8736, http://dx.doi.org/10.1016/j.ceramint.2013.04.058.

[8] M. Sakar, S. Balakumar, P. Saravanan, S. N. Jaisankar, Annealing Temperature Mediated Physical Properties of Bismuth Ferrite ($BiFeO_3$) Nanostructures Synthesized by a Novel Wet Chemical Method, Materials Research Bulletin, Vol. 48, No. 8, 2013, pp. 2878-2885, http://dx.doi.org/10.1016/j.materresbull.2013.04.008.

[9] A. Wrzesinska, A. Khort, I. Bobowska, A. Busiakiewicz, A. W. Puszkarz, Influence of The La^{3+}, Eu^{3+}, and Er^{3+} Doping on Structural, Optical, and Electrical Properties of $BiFeO_3$ Nanoparticles Synthesized by Microwave-Assisted Solution Combustion Method, Journal of Nanomaterials, Vol. 2019, 2019, pp. 1-11, https://doi.org/10.1155/2019/5394325.

[10] X. Li, Z. Zhu, X. Yin, F. Wang, W. Gu, Z. Fu, Y. Lu, Enhanced Magnetism and Light Absorption of Eu-Doped $BiFeO_3$, Journal of Materials Science: Materials in Electronics, Vol. 27, No. 7, 2016, pp. 7079-7083, https://link.springer.com/article/10.1007/s10854-016-4666-3.

[11] T. E. Bahraoui, T. S. Tlemçani, M. Taibi, H. Zaarour, A. E. Bey, A. Belayachi, A. T. Silver, G. Schmerber, A. M. E. Naggar, A. A. Albassam, G. Lakshminarayana, A. Dinia, M. A. Lefdil, Characterization of Multiferroic $Bi_{1-x}Eu_xFeO_3$ Powders Prepared by Sol-Gel Method, Materials Letters, Vol. 182, 2016, pp. 151-154, http://dx.doi.org/10.1016/j.matlet.2016.06.118.

[12] J. Liu, L. Fang, F. Zheng, S. Ju, M. Shen, Enhancement of Magnetization in Eu Doped $BiFeO_3$ Nanoparticles, Applied Physics Letters, Vol. 95, No. 2, 2009, pp. 022511, http://dx.doi.org/10.1063/1.3183580.

[13] V. F. Freitas, H. L. C. Grande, S. N. Medeiros, I. A. Santos, L. F. Cótica, A. A. Coelho, Structural, Microstructural and Magnetic Investigations in High-Energy Ball Milled $BiFeO_3$ and $Bi_{0.95}Eu_{0.05}FeO_3$ Powders, Journal of Alloys and Compounds, Vol. 461, No. 1-2, 2008, pp. 48-52, https://doi.org/10.1016/j.jallcom.2007.07.069.

[14] J. S. Park, Y. J. Yoo, J. S. Hwang, J. H. Kang, B. W. Lee, Y. P. Lee, Enhanced Ferromagnetic Properties in Ho and Ni Co-Doped $BiFeO_3$ Ceramics, Journal of Applied Physics, Vol. 115, No. 1, 2014, pp. 013904, http://dx.doi.org/10.1063/1.4860296.

[15] V. A. Surdu, R. D. Trusca, B. S. Vasile, O. C. Oprea, E. Tanasa, L. Diamandescu, E. Andronescu, A. C. Ianculescu, $Bi_{1-x}Eu_xFeO_3$ Powders: Synthesis, Characterization, Magnetic and Photoluminescence Properties, Nanomaterials (Basel), Vol. 9, No. 10, 2019, pp. 1465, https://doi.org/10.3390/nano9101465.

[16] M. Cazayous, D. Malka, D. Lebeugle, D. Colson, Electric Field Effect on $BiFeO_3$ Single Crystal Investigated by Raman Spectroscopy, Applied Physics Letters, Vol. 91, 2007, pp. 071910, http://dx.doi.org/10.1063/1.2771380.

[17] G. L. Yuan, S. W. Or, H. L. Chan, Raman Scattering Spectra and Ferroelectric Properties of $Bi_{1-x}Nd_xFeO_3$ (x = 0-0.2) Multiferroic Ceramics, Journal of Applied Physics, Vol. 101, 2007, pp. 064101, http://dx.doi.org/10.1063/1.2433709.

[18] Y. Yang, J. Y. Sun, K. Zhu, Y. L. Liu, L. Wan, Structure Properties of $BiFeO_3$ Films Studied by Micro-Raman Scattering, Journal of Applied Physics, Vol. 103, No. 9, 2008, pp. 093532, http://dx.doi.org/10.1063/1.2913198.

[19] T. Kushida, Site-Selective Fluorescence Spectroscopy of Eu^{3+} and Sm^{2+} Ions in Glass, Journal of Luminescence, Vol. 100, 2002, pp. 73-88, https://doi.org/10.1016/S0022-2313(02)00443-X.

[20] D. V. Thang, N. V. Quang, N. M. Hung, L. T. M. Oanh, N. C. Khang, B. D. Tu, D. T. X. Thao, N. V. Minh, Structural, Optical, Ferroelectric and Ferromagnetic Properties of $Bi_{1-x}Gd_xFeO_3$ Materials, Journal of Electronic Materials, Vol. 49, No. 7, 2020, pp. 4443-4449, https://doi.org/10.1007/s11664-020-08158-y.

[21] P. C. Sati, M. Kumar, S. Chhoker, Low Temperature Ferromagnetic Ordering and Dielectric Properties of $Bi_{1-x}Dy_xFeO_3$ Ceramics, Ceramics International, Vol. 41, No. 2, 2015, pp. 3227-3236, http://dx.doi.org/10.1016/j.ceramint.2014.11.012.

[22] P. Suresh, S. Srinath, Study of Structure and Magnetic Properties of Rare Earth Doped $BiFeO_3$, Physica B: Condensed Matter, Vol. 448, 2014, pp. 281-284, http://dx.doi.org/10.1016/j.physb.2014.03.040.